

Multiscale Modeling of Alkali Silica Reaction Deterioration of Concrete Structures

Gianluca Cusatis



NORTHWESTERN
UNIVERSITY

1st Zdeněk P. Bažant (ZPB) FraMCoS Workshop
Berkeley, CA (USA)

May 29, 2016

Acknowledgments

Collaborators

- Mohammed Alnagar, RPI, Troy (NY), USA.
- Jianmin Qu, Tufts University, Boston (MA), USA.
- Roozbeh Rezakhani, Northwestern University, Evanston (IL), USA.
- Daniele Pelessone, Xinwei Zhou, ES3, San Diego (CA), USA.
- Giovanni Di Luzio, Politecnico di Milano, Milan, Italy.

Financial Support

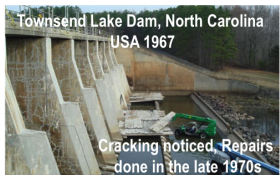
- National Science Foundation (NSF)
- Department of Homeland Security
- Nuclear Regulatory Commission

Presentation Outline

- 1 Introduction
- 2 Alkali Silica Reaction (ASR) Model
- 3 The Lattice Discrete Particle Model (LDPM)
- 4 Numerical Simulations
- 5 Interpretation of Nonlinear Ultrasound Measurements
- 6 Mathematical Homogenization
- 7 Conclusions

Example of Deterioration : Alkali Silica Reaction (ASR)

Dams



Bridges



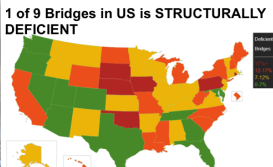
Nuclear Power Plants

Example of Deterioration : Alkali Silica Reaction (ASR)

Dams



Bridges



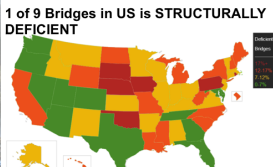
Nuclear Power Plants

Example of Deterioration : Alkali Silica Reaction (ASR)

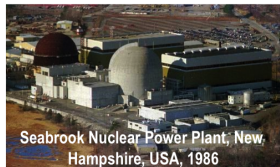
Dams



Bridges

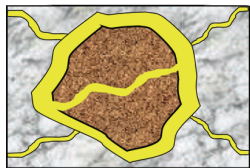
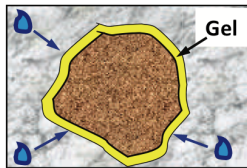
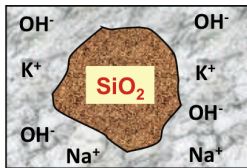


Nuclear Power Plants

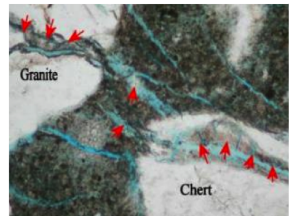
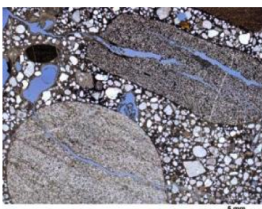
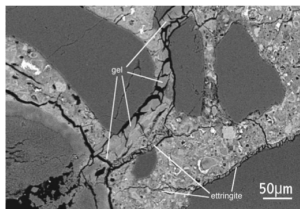


Alkali Silica Reaction (ASR) in a Nutshell

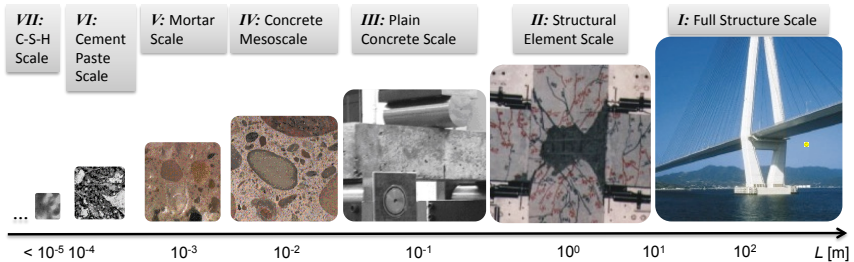
- Chemical Reaction (Very simplistic description)



- Mechanical Deterioration



Concrete is a Multiscale Material

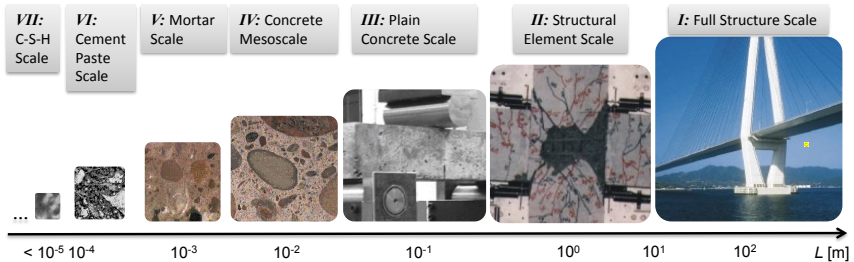


Material Science

Mechanics

Structural
Engineering

Concrete is a Multiscale Material

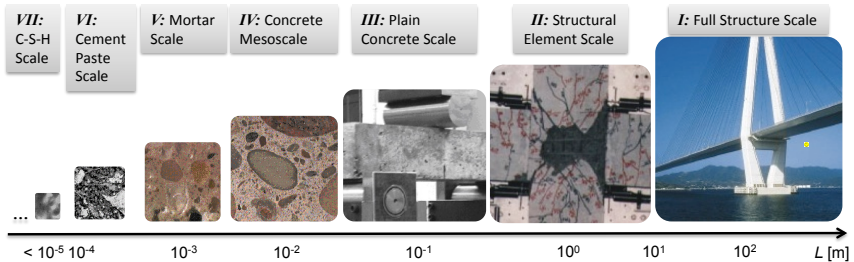


Material Science

Mechanics

Structural
Engineering

Concrete is a Multiscale Material

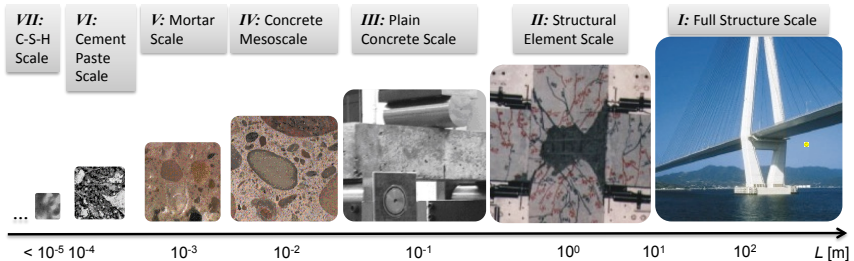


Material Science

Mechanics

Structural
Engineering

Concrete is a Multiscale Material



Material Science

Mechanics

Structural
Engineering

Given

- ① A specific engineering problem and
- ② A fine-scale model of reference

A multiscale model is

an **approximation** of the fine-scale solution characterized by the **max accuracy** for a given **acceptable cost** or the **min cost** for a given **required accuracy**

- *Accuracy* must evaluated against a *Calibrated* and *Validated* fine scale model of reference to avoid “Garbage-down, Garbage-up”
- *Cost* is application and resource dependent.

- **Information Passing** - Discretized subscale material element is embedded into a point of the macro-scale continuum (an integration point of a finite element (e.g. Computational homogenization, mathematical homogenization, microplane model, etc.)
- **Concurrent** - A finite region of the macro-continuum coarse mesh is overlapped or replaced by a fine mesh or discrete sub-structure (meso-structure) model representing the subscale (e.g. Variational multiscale method, bridging scale method, multigrid methods).
- **Coarse-graining** Coarse and fine scale models are both discrete and one particle of the coarse scale simulate the behavior of a certain number of fine-scale particles.

Multiscale Computational Framework

Miniscale

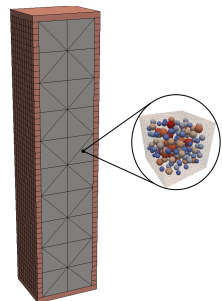
- ASR gel formation
- Water imbibition
- ASR Gel expansion
- Length scale from μm to mm

Mesoscale

- Cracking
- Creep and Shrinkage
- Length scale of mm to cm

Macroscale

- Strength and Stiffness Degradation
- Length scale of cm to m



Presentation Outline

- 1 Introduction
- 2 Alkali Silica Reaction (ASR) Model
- 3 The Lattice Discrete Particle Model (LDPM)
- 4 Numerical Simulations
- 5 Interpretation of Nonlinear Ultrasound Measurements
- 6 Mathematical Homogenization
- 7 Conclusions

Simplifying a very complex phenomenon

- The aggregate particles are assumed to have spherical shape.
- Silica is assumed to be smeared uniformly over the aggregate volume.
- The dissolution of silica is assumed to progress in a uniform manner in the radial direction inward from the surface towards the particle center.
- The expansion of ASR gel is mostly due to water imbibition.
- Continuous supply of water is needed for the swelling to continue over time.

ASR Model :: Gel Formation

Reaction front :

$$\dot{z} = -a_s(h, T)w_e(h, \alpha_c)/[r_w c_s z (1 - \frac{2z}{D})]$$

ASR Gel permeability :

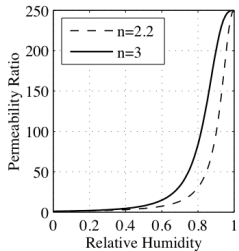
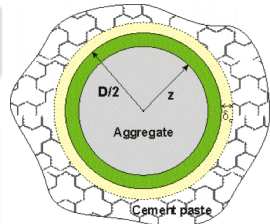
$$a_s = e^{\left(\frac{E_{ag}}{RT_0} - \frac{E_{ag}}{RT}\right)} a_s^1 \left[1 + \left(\frac{a_s^1}{a_s^0} - 1\right) (1 - h)^{n_z}\right]^{-1}$$

ASR Gel Mass :

$$M_g = \kappa_a \frac{\pi}{6} (D^3 - 8z^3) c_s \frac{m_g}{m_s}$$

Effect of Alkali Content :

$$\kappa_a = \min(\langle c_a - c_a^0 \rangle / (c_a^1 - c_a^0), 1)$$



ASR Model :: Gel Formation

Reaction front :

$$\dot{z} = -a_s(h, T)w_e(h, \alpha_c)/[r_w c_s z (1 - \frac{2z}{D})]$$

ASR Gel permeability :

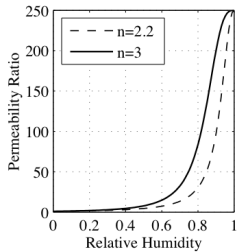
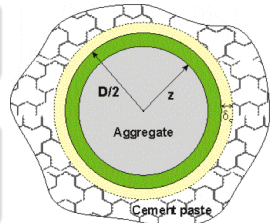
$$a_s = e^{\left(\frac{E_{ag}}{RT_0} - \frac{E_{ag}}{RT}\right)} a_s^1 \left[1 + \left(\frac{a_s^1}{a_s^0} - 1\right) (1 - h)^n z\right]^{-1}$$

ASR Gel Mass :

$$M_g = \kappa_a \frac{\pi}{6} (D^3 - 8z^3) c_s \frac{m_g}{m_s}$$

Effect of Alkali Content :

$$\kappa_a = \min(\langle c_a - c_a^0 \rangle / (c_a^1 - c_a^0), 1)$$



ASR Model :: Gel Formation

Reaction front :

$$\dot{z} = -a_s(h, T)w_e(h, \alpha_c)/[r_w c_s z (1 - \frac{2z}{D})]$$

ASR Gel permeability :

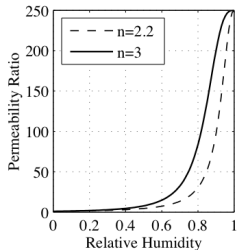
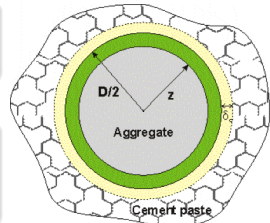
$$a_s = e^{\left(\frac{E_{ag}}{RT_0} - \frac{E_{ag}}{RT}\right)} a_s^1 \left[1 + \left(\frac{a_s^1}{a_s^0} - 1\right) (1 - h)^n z\right]^{-1}$$

ASR Gel Mass :

$$M_g = \kappa_a \frac{\pi}{6} (D^3 - 8z^3) c_s \frac{m_g}{m_s}$$

Effect of Alkali Content :

$$\kappa_a = \min(\langle c_a - c_a^0 \rangle / (c_a^1 - c_a^0), 1)$$



Reaction front :

$$\dot{z} = -a_s(h, T)w_e(h, \alpha_c)/[r_w c_s z \left(1 - \frac{2z}{D}\right)]$$

ASR Gel permeability :

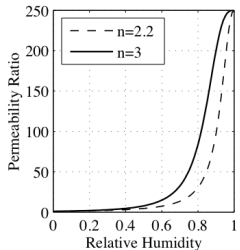
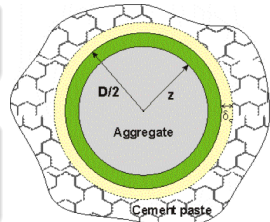
$$a_s = e^{\left(\frac{E_{ag}}{RT_0} - \frac{E_{ag}}{RT}\right)} a_s^1 \left[1 + \left(\frac{a_s^1}{a_s^0} - 1\right) (1-h)^n z\right]^{-1}$$

ASR Gel Mass :

$$M_g = \kappa_a \frac{\pi}{6} (D^3 - 8z^3) c_s \frac{m_g}{m_s}$$

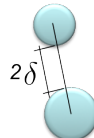
Effect of Alkali Content :

$$\kappa_a = \min(\langle c_a - c_a^0 \rangle / (c_a^1 - c_a^0), 1)$$



Driving force (Thermodynamic Affinity) :

$$A_i = \kappa_i^0 \exp\left(\frac{E_{ai}}{RT_0} - \frac{E_{ai}}{RT}\right) M_g - M_i$$



Imbibition Characteristic time :

$$\tau_i = \delta^2 / C_i$$

Water Imbibition Coefficient :

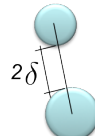
$$C_i = C_i^1 \exp(-\eta M_i) (1 + (C_i^1/C_i^0 - 1)(1 - h)^{n_M})^{-1}$$

Water Imbibition Rate :

$$\dot{M}_i = A_i / \tau_i$$

Driving force (Thermodynamic Affinity) :

$$A_i = \kappa_i^0 \exp\left(\frac{E_{ai}}{RT_0} - \frac{E_{ai}}{RT}\right) M_g - M_i$$



Imbibition Characteristic time :

$$\tau_i = \delta^2 / C_i$$

Water Imbibition Coefficient :

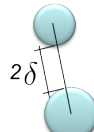
$$C_i = C_i^1 \exp(-\eta M_i) (1 + (C_i^1/C_i^0 - 1)(1 - h)^{n_M})^{-1}$$

Water Imbibition Rate :

$$\dot{M}_i = A_i / \tau_i$$

Driving force (Thermodynamic Affinity) :

$$A_i = \kappa_i^0 \exp\left(\frac{E_{ai}}{RT_0} - \frac{E_{ai}}{RT}\right) M_g - M_i$$



Imbibition Characteristic time :

$$\tau_i = \delta^2 / C_i$$

Water Imbibition Coefficient :

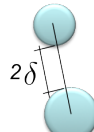
$$C_i = C_i^1 \exp(-\eta M_i) (1 + (C_i^1 / C_i^0 - 1)(1 - h)^{n_M})^{-1}$$

Water Imbibition Rate :

$$\dot{M}_i = A_i / \tau_i$$

Driving force (Thermodynamic Affinity) :

$$A_i = \kappa_i^0 \exp\left(\frac{E_{ai}}{RT_0} - \frac{E_{ai}}{RT}\right) M_g - M_i$$



Imbibition Characteristic time :

$$\tau_i = \delta^2 / C_i$$

Water Imbibition Coefficient :

$$C_i = C_i^1 \exp(-\eta M_i) (1 + (C_i^1 / C_i^0 - 1)(1 - h)^{n_M})^{-1}$$

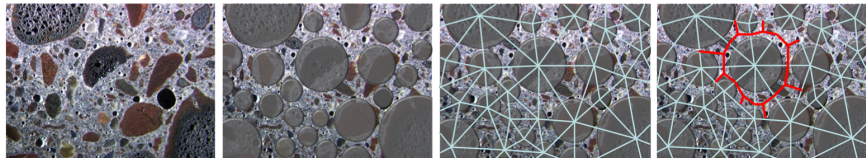
Water Imbibition Rate :

$$\dot{M}_i = A_i / \tau_i$$

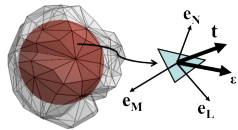
Presentation Outline

- 1 Introduction
- 2 Alkali Silica Reaction (ASR) Model
- 3 The Lattice Discrete Particle Model (LDPM)
- 4 Numerical Simulations
- 5 Interpretation of Nonlinear Ultrasound Measurements
- 6 Mathematical Homogenization
- 7 Conclusions

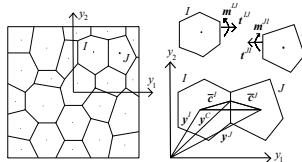
- Geometry



- 3D cell



- Discrete compatibility



Facet Strains

$$\epsilon_\alpha = \frac{1}{r} [\![\mathbf{u}_C]\!] \cdot \mathbf{e}_\alpha; \quad [\![\mathbf{u}_C]\!] = \frac{1}{r} \left(\mathbf{U}^J + \boldsymbol{\Theta}^J \times \mathbf{c}^J - \mathbf{U}^I - \boldsymbol{\Theta}^I \times \mathbf{c}^I \right)$$

Constitutive Laws

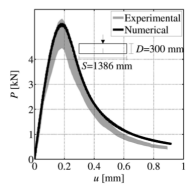
- Fracture and cohesion due to tension and tension-shear
 - $\varepsilon = \sqrt{\varepsilon_N^2 + \alpha(\varepsilon_M^2 + \varepsilon_L^2)}$, $t = \sqrt{t_N^2 + (t_M + t_L)^2/\alpha}$
 - $t_N = (t/\varepsilon)\varepsilon_N$; $t_M = \alpha(t/\varepsilon)\varepsilon_M$; $t_L = \alpha(t/\varepsilon)\varepsilon_L$.
 - $\sigma_{bt} = \sigma_0(\omega) \exp[-H_0(\omega)\langle\varepsilon - \varepsilon_0(\omega)\rangle/\sigma_0(\omega)]$;
- Compaction and pore collapse from compression
 - $-\sigma_{bc}(\varepsilon_D, \varepsilon_V) \leq t_N \leq 0$; $\sigma_{bc} = \sigma_{c0} + \langle -\varepsilon_V - \varepsilon_{c0} \rangle H_c(r_{DV})$;
- Frictional Behavior
 - $\dot{t}_M = E_T(\dot{\varepsilon}_M - \dot{\varepsilon}_M^p)$ $\dot{t}_L = E_T(\dot{\varepsilon}_L - \dot{\varepsilon}_L^p)$;
 - $\varphi = \sqrt{t_M^2 + t_L^2} - \sigma_{bs}(t_N)$
 - $\sigma_{bs} = \sigma_s + (\mu_0 - \mu_\infty)\sigma_{N0}[1 - \exp(t_N/\sigma_{N0})] - \mu_\infty t_N$

Translational and rotational equilibrium equations of each particle

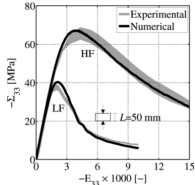
$$M_u^I \ddot{\mathbf{U}}^I - V^I \mathbf{b}^0 = \sum_{\mathcal{F}_I} A \mathbf{t}^{IJ}; \quad M_\theta^I \ddot{\boldsymbol{\Theta}}^I = \sum_{\mathcal{F}_I} A (\mathbf{c}^I \times \mathbf{t}^{IJ} + \mathbf{m}^{IJ})$$

LDPM :: Some Results

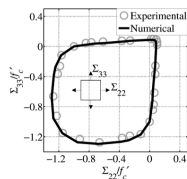
Tensile Fracture



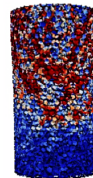
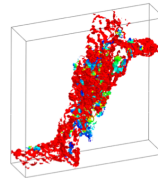
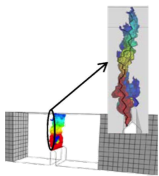
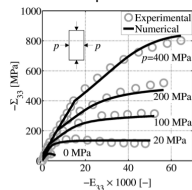
Unconfined Compression



Biaxial Loading



Triaxial Compression



Unconfined Compression, Cont.

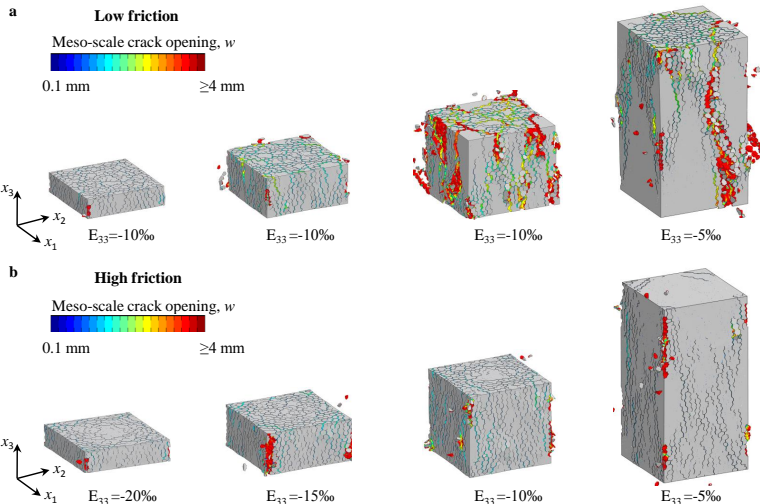


Figure: Unconfined compressive behavior. a) Contours of meso-scale crack opening at failure for low friction boundary conditions; b) Contours of meso-scale crack opening at failure for high friction boundary conditions

Unconfined Compression, Cont.

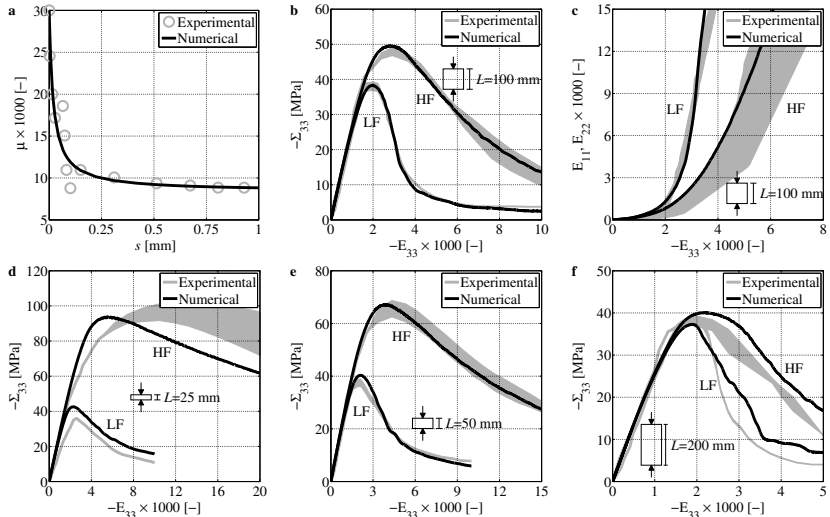
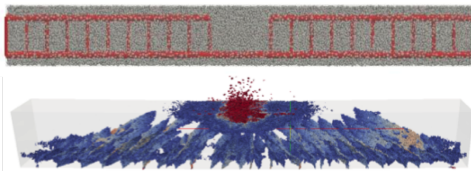
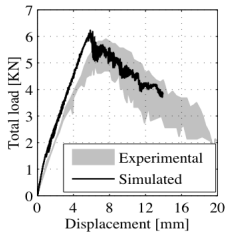
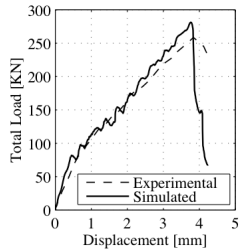


Figure: a) Low friction coefficient $\mu(s) = \mu_d + (\mu_s - \mu_d)s_0/(s_0 + s)$, $\mu_s = 0.03$, $\mu_d = 0.0084$, and $s_0 = 0.0195\text{ mm}$; b) Stress-strain curves for cubes; c) Lateral expansion for cubes; d) Stress-strain curves for very short prisms; e) Stress-strain curves for short prisms; f) Stress-strain curves for long prisms.

Over Reinforced Beam



Deep Beam in Shear



- Radius increase of each aggregate particle

$$r_i = \left(\frac{3M_i}{4\pi\rho_w} + r^3 \right)^{1/3} - r$$

- Normal meso-scale eigenstrain**

$$e_N^a = \langle (r_{i1} + r_{i2})/2 - \delta_c \rangle / \ell \text{ and } \dot{e}_N^a = 0 \text{ for } \zeta = 0$$

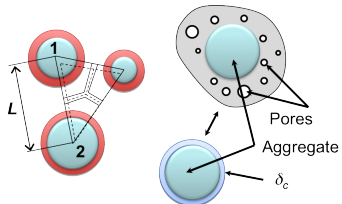
- $e_M^a = e_L^a = 0 \rightarrow \epsilon^a = [e_N^a \ 0 \ 0]^T$

- Incremental LDPM strain**

$$\Delta\epsilon^* = \Delta\epsilon - \Delta\epsilon^a$$

Limitations. The formulation does not account explicitly for ...

- ... the actual chemistry of gel formation.
- ... multi ion transport.
- ... gel expansion into pores and cracks.
- ... non-uniform silica distribution within the aggregate.
- ... local water diffusion through (a) pores, (b) cracks; and (c) gel.



- Radius increase of each aggregate particle $r_i = \left(\frac{3M_i}{4\pi\rho_w} + r^3 \right)^{1/3} - r$

$$r_i = \left(\frac{3M_i}{4\pi\rho_w} + r^3 \right)^{1/3} - r$$

- Normal meso-scale eigenstrain**

$$e_N^a = \langle (r_{i1} + r_{i2})/2 - \delta_c \rangle / \ell \text{ and } \dot{e}_N^a = 0 \text{ for } \zeta = 0$$

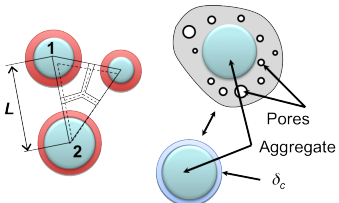
- $e_M^a = e_L^a = 0 \rightarrow \epsilon^a = [e_N^a \ 0 \ 0]^T$

- Incremental LDPM strain**

$$\Delta\epsilon^* = \Delta\epsilon - \Delta\epsilon^a$$

Limitations. The formulation does not account explicitly for ...

- ... the actual chemistry of gel formation.
- ... multi ion transport.
- ... gel expansion into pores and cracks.
- ... non-uniform silica distribution within the aggregate.
- ... local water diffusion through (a) pores, (b) cracks; and (c) gel.



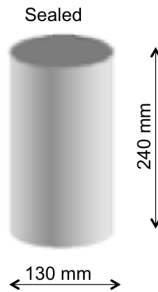
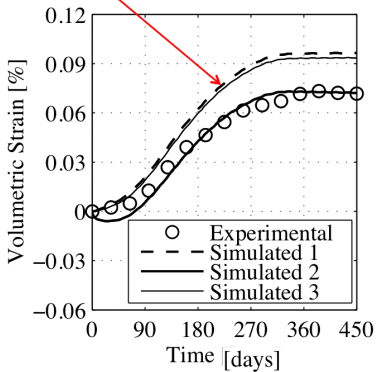
Presentation Outline

- 1 Introduction
- 2 Alkali Silica Reaction (ASR) Model
- 3 The Lattice Discrete Particle Model (LDPM)
- 4 Numerical Simulations
- 5 Interpretation of Nonlinear Ultrasound Measurements
- 6 Mathematical Homogenization
- 7 Conclusions

Model Calibration

Data by S. Multon and F. Toutlemonde, 2006. Cement and Concrete Research, 36:912-920.

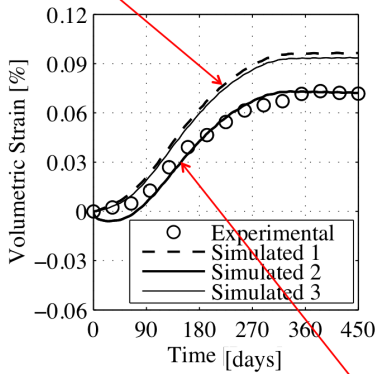
Simulated 1 : No Creep nor Shrinkage



Model Calibration

Data by S. Multon and F. Toutlemonde, 2006. Cement and Concrete Research, 36:912-920.

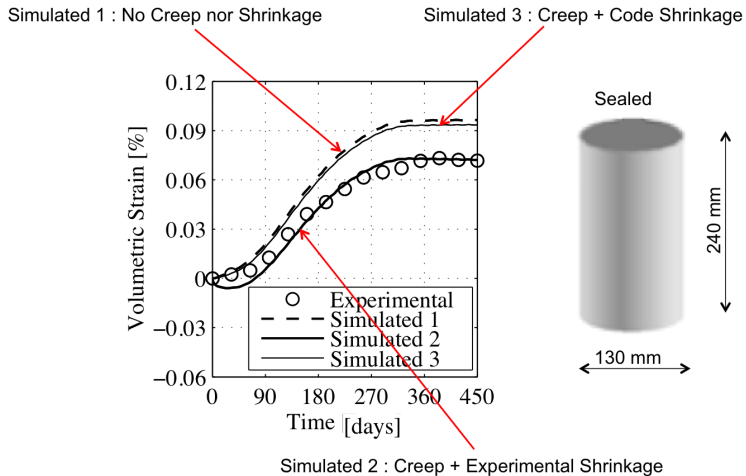
Simulated 1 : No Creep nor Shrinkage



Simulated 2 : Creep + Experimental Shrinkage

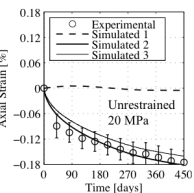
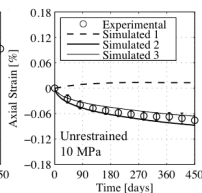
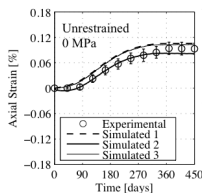
Model Calibration

Data by S. Multon and F. Toutlemonde, 2006. Cement and Concrete Research, 36:912-920.



Validation :: Stress Effect - Axial Stresses

Vertical applied stress:
0, 10, 20 MPa

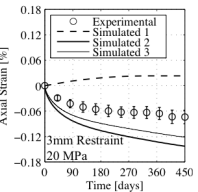
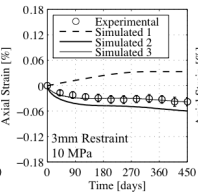
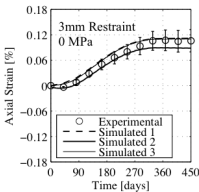
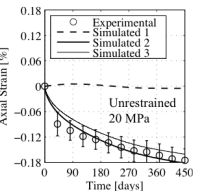
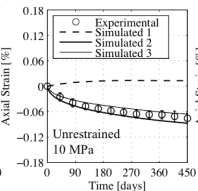
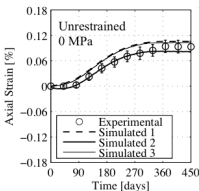


Validation :: Stress Effect - Axial Stresses

Vertical applied stress:
0 , 10 , 20 MPa

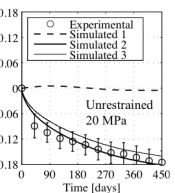
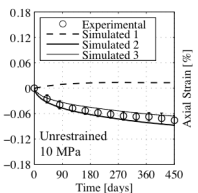
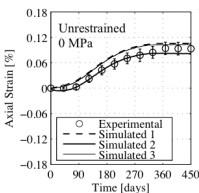


Vertical applied stress:
0 , 10 , 20 MPa

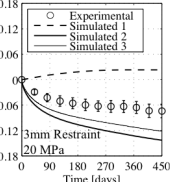
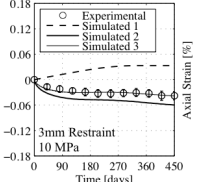
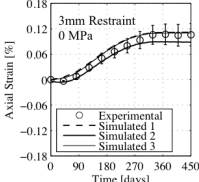


Validation :: Stress Effect - Axial Stresses

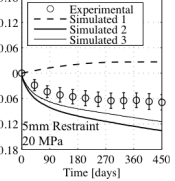
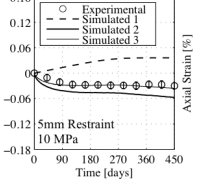
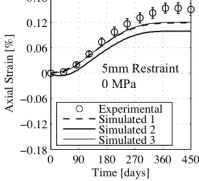
Vertical applied stress:
0 , 10 , 20 MPa



Vertical applied stress:
0 , 10 , 20 MPa



Vertical applied stress:
0 , 10 , 20 MPa



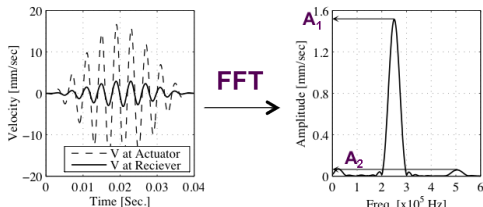
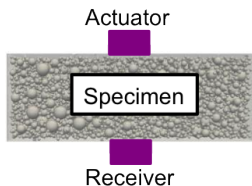
Animation of Damage Evolution

- Free Expansion
- 20 MPa / Unrest.
- 00 MPa / Rest.

Presentation Outline

- 1 Introduction
- 2 Alkali Silica Reaction (ASR) Model
- 3 The Lattice Discrete Particle Model (LDPM)
- 4 Numerical Simulations
- 5 Interpretation of Nonlinear Ultrasound Measurements
- 6 Mathematical Homogenization
- 7 Conclusions

Nonlinear Acoustic Nonlinearity Techniques



1D nonlinear wave propagation

$$\frac{\partial^2 u}{\partial t^2} = c^2 \frac{\partial^2 u}{\partial X^2} \left(1 + \beta \frac{\partial u}{\partial X} \right)$$

Single harmonic plane wave

$$A_1 \cos(kX - \omega t)$$

Solution with perturbation analysis

$$\begin{aligned} u &= -\frac{1}{8}\beta k^2 A_1^2 X + A_1 \cos(kX - \omega t) + \frac{1}{8}\beta k^2 A_1^2 X \cos[2(kX - \omega t)] + \dots \\ &= A_0 + A_1 \cos(kX - \omega t) + A_2 \cos[2(kX - \omega t)] + \dots \end{aligned}$$

Acoustic Nonlinearity Parameter (ANLP)

$$\beta = \frac{8A_2}{k^2 L A_1^2} \propto A_2/A_1^2$$

How does it relate to damage?

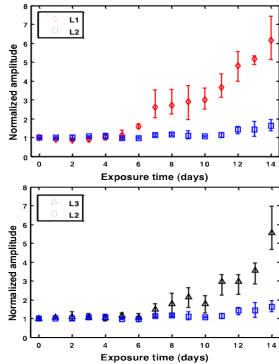
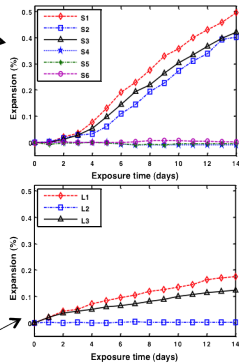
Accelerated Mortar Bar Test with ANLP testing



1" x 1" x 10"



4" x 4" x 10"



Alkali Ion Macro Diffusion

Nonlinear Alkali ion diffusion model

$$\frac{dc_i}{dt} = \nabla \cdot (D_i(c_i) \nabla c_i) \text{ With } D_i(c_i) = D_i^1 \left[1 + \left(\frac{D_i^1}{D_i^0} - 1 \right) \left\langle 1 - \frac{c_i}{c_i^{max}} \right\rangle^{n_i} \right]^{-1}$$

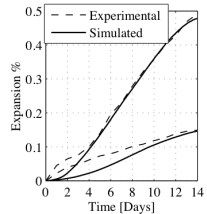
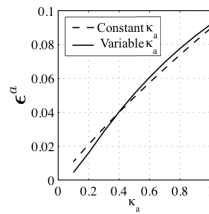
- Modification of ASR-LDPM for Variable Alkali Content

Reaction Front :

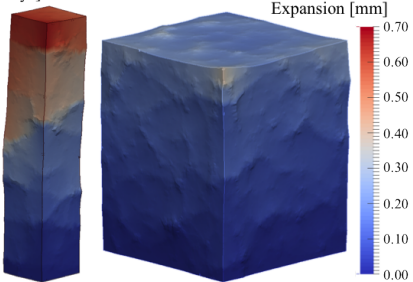
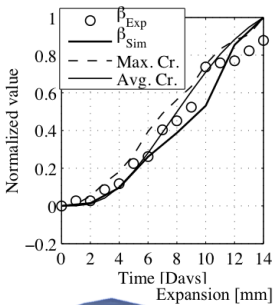
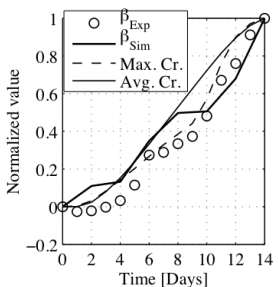
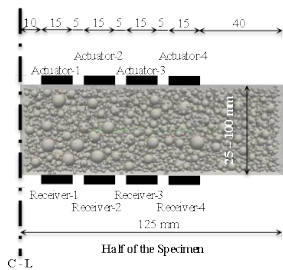
$$z_\kappa = -\frac{a_s(T) w_s \sqrt[3]{\kappa_a}}{r_w c_s z_\kappa \left(1 - \frac{2z_\kappa}{D}\right)}, \quad z_\kappa = z \sqrt[3]{\kappa_a}$$

Total Mass of Gel per Aggregate :

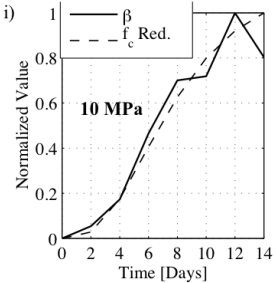
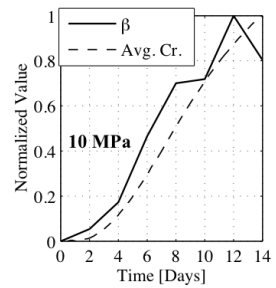
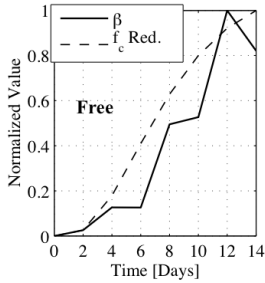
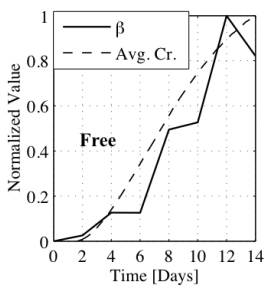
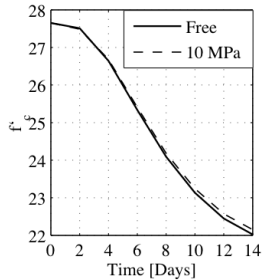
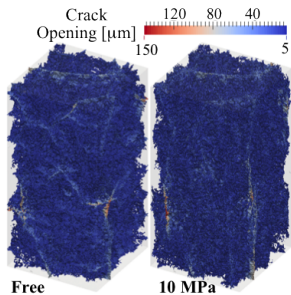
$$M_g = \frac{\pi D^3}{6} \left(\kappa_a - \left(\frac{2z_\kappa}{D} \right)^3 \right) c_s \frac{m_g}{m_s}$$



Numerical Simulation of ANLP



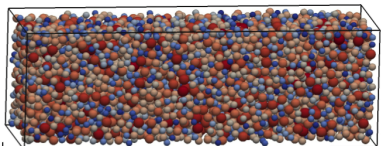
Parametric Analysis



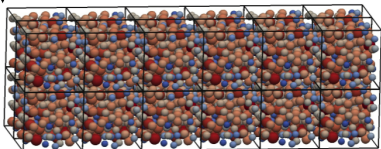
Presentation Outline

- 1 Introduction
- 2 Alkali Silica Reaction (ASR) Model
- 3 The Lattice Discrete Particle Model (LDPM)
- 4 Numerical Simulations
- 5 Interpretation of Nonlinear Ultrasound Measurements
- 6 Mathematical Homogenization
- 7 Conclusions

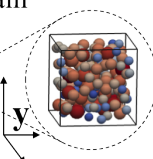
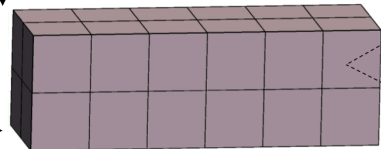
Separation of Scales



Periodicity of particle distribution



FE representation of Macro domain



- Separation of scales

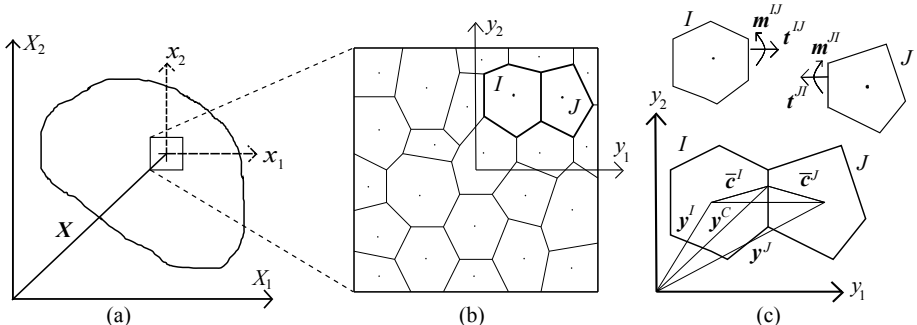
$$\mathbf{x} = \eta \mathbf{y}$$

$$0 < \eta \ll 1$$

- \mathbf{x} is the coarse scale coordinate system
- \mathbf{y} is the fine scale coordinate system

RVE problem at each macroscopic Gauss point

Asymptotic Expansion



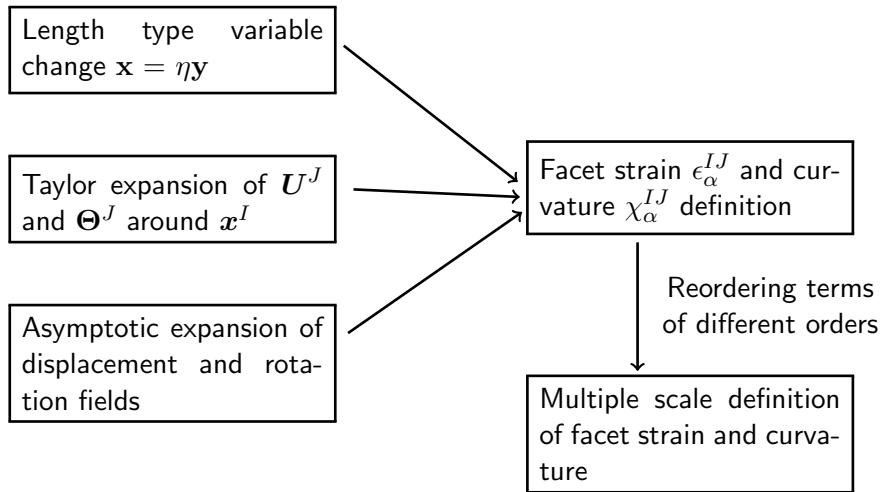
- Asymptotic expansion of particle displacement

$$\mathbf{u}(\mathbf{x}, \mathbf{y}) \approx \mathbf{u}^0(\mathbf{x}, \mathbf{y}) + \eta \mathbf{u}^1(\mathbf{x}, \mathbf{y})$$

- Asymptotic expansion of particle rotation

$$\theta(\mathbf{x}, \mathbf{y}) \approx \eta^{-1} \boldsymbol{\omega}^0(\mathbf{x}, \mathbf{y}) + \boldsymbol{\varphi}^0(\mathbf{x}, \mathbf{y}) + \boldsymbol{\omega}^1(\mathbf{x}, \mathbf{y}) + \eta \boldsymbol{\varphi}^1(\mathbf{x}, \mathbf{y})$$

Several Pages of Mathematical Manipulations

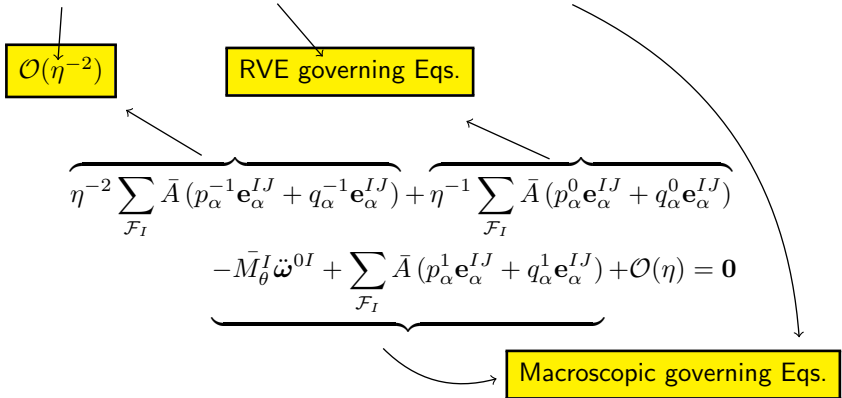


$$\epsilon_\alpha = \eta^{-1} \epsilon_\alpha^{-1} + \epsilon_\alpha^0 + \eta \epsilon_\alpha^1$$

$$\eta \chi_\alpha = \eta^{-1} \psi_\alpha^{-1} + \psi_\alpha^0 + \eta \psi_\alpha^1$$

Multiple Scale Equilibrium Equations

$$\underbrace{\eta^{-2} \sum_{\mathcal{F}_I} \bar{A} t_\alpha^{-1} \mathbf{e}_\alpha^{IJ}}_{\mathcal{O}(\eta^{-2})} + \underbrace{\eta^{-1} \sum_{\mathcal{F}_I} \bar{A} t_\alpha^0 \mathbf{e}_\alpha^{IJ}}_{\text{RVE governing Eqs.}} + \underbrace{\sum_{\mathcal{F}_I} \bar{A} t_\alpha^1 \mathbf{e}_\alpha^{IJ} - \bar{M}_u^I \ddot{\mathbf{u}}^{0I} + \bar{V}^I \mathbf{b}^0}_{-\bar{M}_u^I \ddot{\mathbf{u}}^{0I} + \bar{V}^I \mathbf{b}^0 + \mathcal{O}(\eta)} = \mathbf{0}$$



Rigid Body Motion

- Considering facet level elastic constitutive law along with $\mathcal{O}(\eta^{-2})$
 - \mathbf{u}^0 and $\boldsymbol{\omega}^0$ are rigid body motion and rotation of the RVE
 - $u_i^0(\mathbf{x}, \mathbf{y}) = v_i^0(\mathbf{x}) + \varepsilon_{ijk} y_k \omega_j^0(\mathbf{x})$
 - revise facet strain and curvature definition $\epsilon_\alpha = \epsilon_\alpha^0 + \eta \epsilon_\alpha^1$; $\eta \chi_\alpha = \psi_\alpha^0 + \eta \psi_\alpha^1$

Fine-scale displacement jump

$$\gamma_{ij} = v_{j,i}^0 - \varepsilon_{ijk} \omega_k^0$$

$$\epsilon_\alpha^0 = \bar{r}^{-1} \left(\underbrace{u_i^{1J} - u_i^{1I} + \varepsilon_{ijk} \omega_j^{1J} \bar{c}_k^J - \varepsilon_{ijk} \omega_j^{1I} \bar{c}_k^I}_{\text{displacement jump}} \right) e_{\alpha i}^{IJ} + P_{ij}^\alpha (\gamma_{ij} + \varepsilon_{jmn} \kappa_{im} y_n^c)$$

$$\psi_\alpha^0 = \bar{r}^{-1} \left(\underbrace{\omega_i^{1J} - \omega_i^{1I}}_{\text{rotation jump}} \right) e_{\alpha i}^{IJ} + P_{ij}^\alpha \kappa_{ij}$$

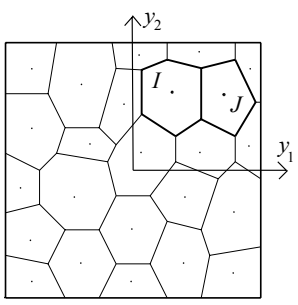
Fine-scale rotation jump

$$\kappa_{ij} = \omega_{j,i}^0$$

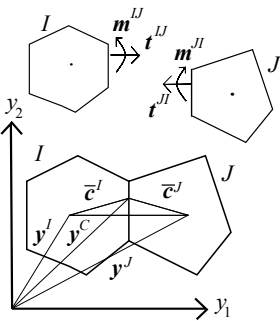
$P_{ij}^\alpha = n_i^{IJ} e_{\alpha j}^{IJ}$ is the projection operator

- Terms of $\mathcal{O}(\eta^{-1})$ state RVE equilibrium equations
 - Force equilibrium equation
 - Moment equilibrium equation

$$\sum_{\mathcal{F}_I} A t_\alpha^0 \mathbf{e}_\alpha^{IJ} = 0$$



$$\sum_{\mathcal{F}_I} A (\mathbf{c}^I \times t_\alpha^0 \mathbf{e}_\alpha^{IJ} + m_\alpha^0 \mathbf{e}_\alpha^{IJ}) = 0$$



Macroscopic Governing Equations

- Terms of $\mathcal{O}(\eta^0)$ state macroscopic equilibrium equations
 - Macroscopic translational equation of motion

$$M_u^I \ddot{u}_i^{0I} = \eta \sum_{\mathcal{F}_I} A \frac{\partial t_i^{IJ}}{\partial \epsilon_\alpha^0} \epsilon_\alpha^1 + V^I b_i^0$$

↓
Sum over all particles and divide by
the RVE volume and some
mathematical work

$$\rho_u \ddot{v}_i^0 = \sigma_{ji,j}^0 + b_i \quad ; \quad \sigma_{ij}^0 = \frac{1}{2V_0} \sum_I \sum_{\mathcal{F}_I} A r_\alpha^0 P_{ij}^\alpha$$

$$\rho_u = \sum_I M_u^I / V_0 \text{ mass density of the macroscopic continuum}$$

Macroscopic Governing Equations

- Terms of $\mathcal{O}(\eta^0)$ state macroscopic equilibrium equations
 - Macroscopic rotational equation of motion

$$M_u^I \varepsilon_{ijk} X_j^I (\ddot{v}_k^0 + \varepsilon_{kmn} \eta^{-1} \ddot{\omega}_m^0 x_n^I) + \eta^{-1} M_\theta^I \ddot{\omega}_i^0 = \eta \sum_{\mathcal{F}_I} A \left(\frac{\partial w_i^{IJ}}{\partial \epsilon_\alpha^0} \epsilon_\alpha^1 + \frac{\partial m_i^{IJ}}{\partial \psi_\alpha^0} \psi_\alpha^1 \right) + V^I \varepsilon_{ijk} X_j^I b_k^0$$

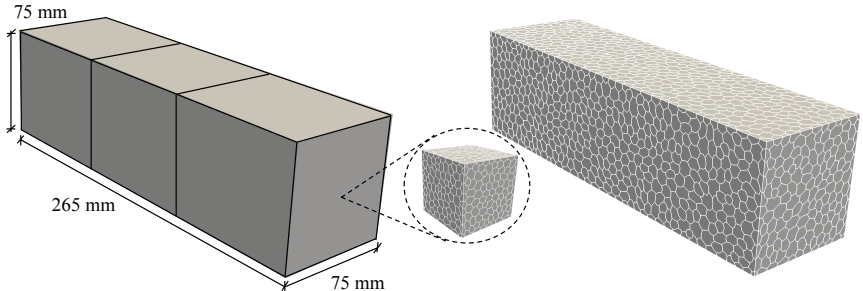


Sum over all particles and divide by
the RVE volume and some
mathematical work

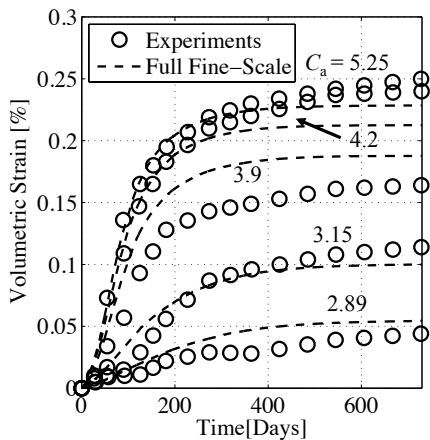
$$\rho_{\theta ij} (\eta^{-1} \ddot{\omega}_j^0) = \varepsilon_{ijk} \sigma_{ij}^0 + \frac{\partial \mu_{ji}^0}{\partial x_j} ; \quad \mu_{ij}^0 = \frac{1}{2V_0} \sum_I \sum_{\mathcal{F}_I} Ar(m_\alpha^0 P_{ij}^\alpha + t_\alpha^0 Q_{ij}^\alpha)$$

$$\rho_{im}^\theta = \sum_I [M_\theta^I \delta_{im} + M_u^I \varepsilon_{ijk} \varepsilon_{kmn} x_j^I x_n^I] / V_0 : \text{the inertia tensor of the unit cell}$$

$$Q_{ij}^\alpha = n_i^{IJ} \varepsilon_{jkl} x_k^C e_{\alpha l}^{IJ} : \text{projection tensor}$$

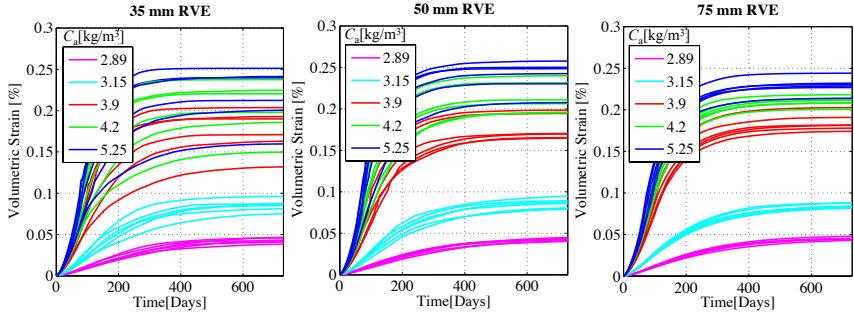


(Left) Two-scale homogenization problem. (Right) Full mesoscale prism model.

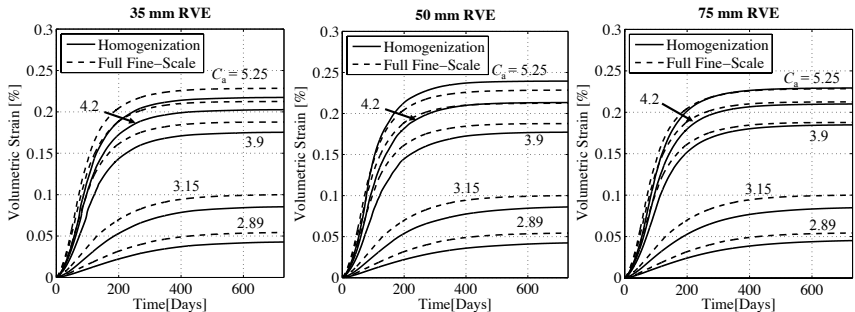


Volumetric expansion of concrete prism for different alkali contents by experiment and full fine-scale analysis.

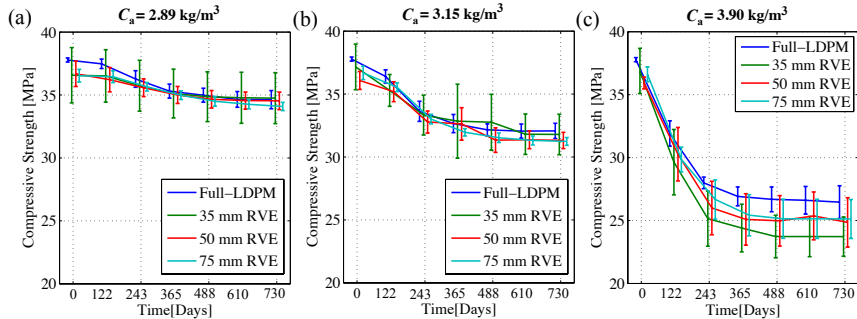
ASR and Homogenization :: Effect of RVE Size



Volumetric expansion using RVE size of (left) 35 mm (center) 50 mm, and (right) 75 mm.

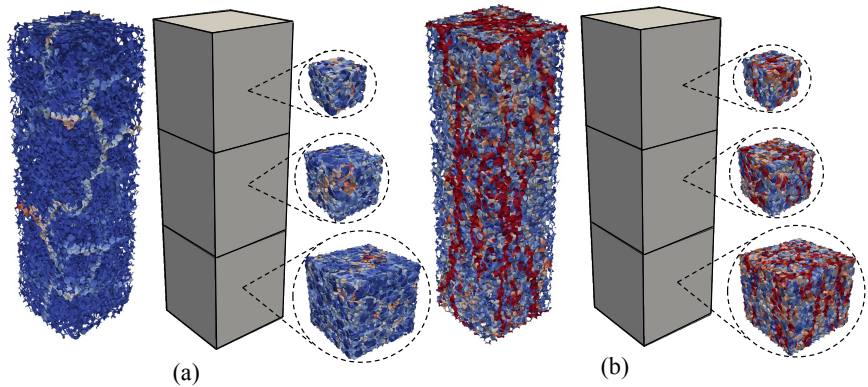


Comparison of the homogenization results using different RVE sizes with the full fine-scale ones.

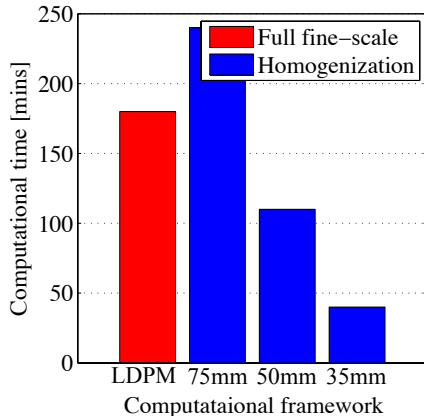


Comparison of the compressive strength obtained by the full fine-scale simulation and the homogenization framework.

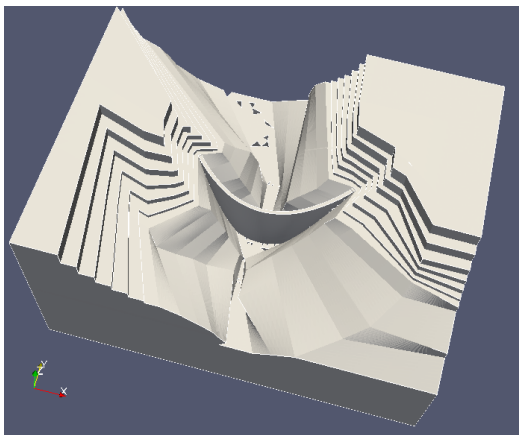
ASR and Homogenization :: Crack Patterns



Crack opening contour of the concrete prism and RVEs of different sizes under (a) free expansion due to ASR effect with $C_a = 3.9 \text{ kg/m}^3$ and (b) uniaxial compression after ASR expansion.



Computational cost in full fine-scale analysis and homogenization framework with different RVE sizes.

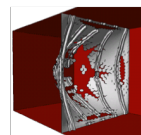
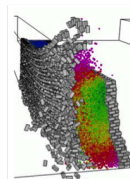
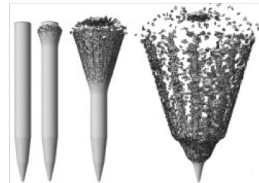


Full scale dam analysis ...

MARS (Modeling and Analysis of the Response of Structures) is a multipurpose object-oriented computational software for simulating the mechanical response of structural systems subjected to short duration events.

It is based on dynamic explicit algorithms and it implements all the capabilities and versatility of a general finite element code.

<http://mars.es3inc.com/>



Presentation Outline

- 1 Introduction
- 2 Alkali Silica Reaction (ASR) Model
- 3 The Lattice Discrete Particle Model (LDPM)
- 4 Numerical Simulations
- 5 Interpretation of Nonlinear Ultrasound Measurements
- 6 Mathematical Homogenization
- 7 Conclusions

- Alkali Silica Reaction is a complex multiscale-multiphysics phenomenon affecting the deterioration of concrete structures worldwide.
- Predictive computational models are needed to evaluate existing deteriorated structures.
- A multi scale framework was proposed to simulate ASR deterioration within the LDPM framework.
- LDPM can be extended effectively to account for various aging and deterioration phenomena.
- Classical mathematical homogenization can be used to upscale LDPM response for durability related structural analysis.
- All LDPM-based algorithms are currently implemented in the commercially available MARS software – www.mars.es3inc.com

Free time with my students



NORTHWESTERN
UNIVERSITY